A Microwave Channelizer and Spectroscope Based on an Integrated Optical Bragg-Grating Fabry–Perot and Integrated Hybrid Fresnel Lens System

Steve T. Winnall, *Member, IEEE*, A. C. Lindsay, *Member, IEEE*, Michael W. Austin, *Member, IEEE*, John Canning, *Member, IEEE*, and Arnan Mitchell, *Member, IEEE*

Abstract—A compact means to separate microwave and millimeter-wave optical signals by RF frequency in real time is demonstrated. The approach is to employ an integrated optical Bragg grating Fabry–Perot (BGFP) device to spatially separate optically modulated microwave signals with high resolution. The compactness is achieved through the use of an integrated optical hybrid diffractive lens beam expander to provide the required optical wavefront to the BGFP. A proof-of-principle measurement was performed from 1 to 23 GHz with peak finesse of 27. The theoretical analysis, fabrication procedure, experimental results, limitations, and improvements are described.

Index Terms—Fabry–Perot interferometers, optical planar waveguide components, optical signal processing, microwave receivers.

I. INTRODUCTION

RF SIGNALS may be separated into many contiguous parallel channels using optical demultiplexers with high resolving power. These devices are described as channelizers, and have applications such as microwave signal estimation [1]. Such separation of a wide microwave spectrum into smaller frequency channels provides continuous spectral coverage suitable for electronic analog-to-digital conversion [2]. Apart from microwave channelizers, such devices are envisaged for ultra-narrow wavelength division multiplexing (WDM) [3], real-time optical spectrum analysis [4], and wavelength references [5]. Many optical channelizer approaches have been attempted. Acoustooptic channelizers are limited to below a few gigahertz due to phonon scattering, but have been demonstrated in integrated optical form [6], [7]. Integrated magnetooptic devices such as presented in [8] offer higher frequencies of operation at the expense of narrow bandwidth and high microwave drive levels. Passive integrated optical devices such as Bragg gratings, ring resonators, and Mach–Zehnder interferometers
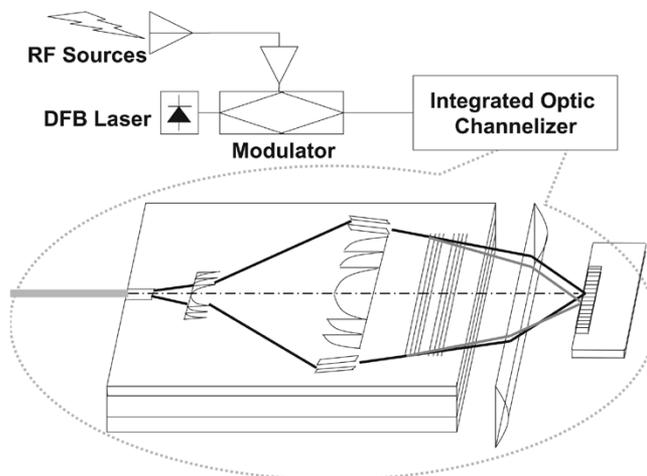
Fig. 1.   Channelizer architecture.

might appear suitable for such applications. These devices, however, are limited in resolving power [9], cascaded power loss in reflection [10], interferometer limitations [11], complex optical post-tuning steps [12]–[14], and bulky classical optical implementation [15], [16]. Recent developments in the literature show a possibility of resolving power and small footprint attributable to multibeam interferometers [17], [18]. The approach described in this paper is based upon spatial wavelength demultiplexing using the Fabry–Perot etalon [19]. Early studies have demonstrated the feasibility of this approach, but in bulky classical optical form [20], [21].

The authors present for the first time a compact integrated optical channelizer based on a Bragg grating Fabry–Perot (BGFP) etalon. The incident wavefront to the Fabry–Perot is diffracted by integrated optical hybrid lens structures. The device is compact, is easy to mass produce, and has the potential for high resolving power and wide microwave bandwidth.

II. SYSTEM DESCRIPTION

A. BGFP Channelizer

The architecture is depicted in Fig. 1. A wide-band electrooptical modulator allows a microwave or millimeter-wave signal to modulate an optical carrier that is delivered via fiber to the integrated optical device. In this device, the optical phase front is expanded and the integrated optical lens system causes this signal to diverge laterally. A Fabry–Perot etalon
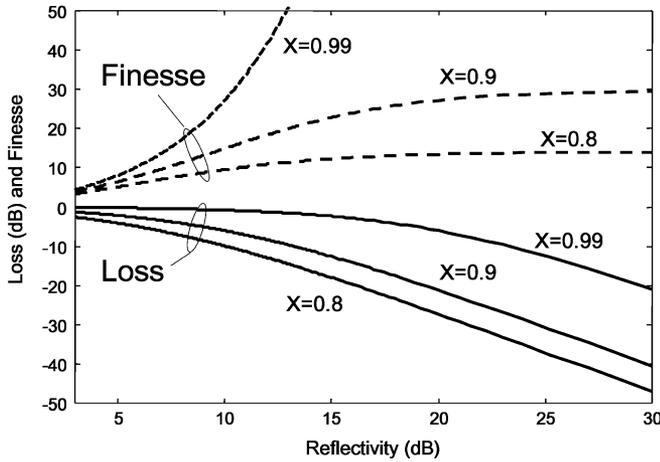
Fig. 2. Loss and finesse versus reflectivity.

formed with two Bragg gratings acts upon this wavefront to create a resonance condition that is now a function of angle and wavelength—thus providing microwave channelization.

An array of low-speed photodetectors at the focal plane then provides N frequency resolved outputs. Wide bandwidth microwave and millimeter-wave operation is possible since the modulation and dispersion functions are separate. Modulation over 40 GHz with low-drive power is possible [22], and 100 channels are feasible based on published Fabry–Perot performance [23].

B. Departure From Ideal Performance

The relationship between the number of channels and the microwave bandwidth is defined by the Fabry–Perot *finesse*, typically 10–100 in the etalon configuration. Reduced finesse directly reduces the RF frequency resolution. Physical effects impacting on the BGFP finesse are, therefore, analyzed here. The BGFP is made up of wavelength-dependent reflectors and contains a lossy cavity element—these departures from ideal performance place a limit on the finesse achievable. To this end, the ideal power transmission through the BGFP can be described in terms of a wavelength-dependent reflectivity $R(\delta)$ and a single-pass cavity transmission X as

$$P_{X,R}(\delta) = \frac{X\left(1 - R(\delta)\right)^2}{\left(1 - XR(\delta)\right)^2 + 4R(\delta)X\sin^2(\delta/2)} \quad (1)$$

where δ is a dispersion detuning parameter dependent on wavelength, cavity spacing, and angle into the etalon [21]. Fig. 2 illustrates the loss and resultant finesse associated with a practical device and, therefore, the upper limit on reflectivity if X is known. It should be noted that this loss is in addition to the fundamental loss that occurs due to spreading of the incident beam into angular resolution elements.

Other effects have the potential to reduce the frequency resolution. Fortunately the incident angle to the Bragg grating is insufficient to reduce the reflection dramatically [24]. In a classical etalon, finesse is limited by defects such as dust, pressure, and etalon plate flatness and curvature. In the integrated optical device, these defects manifest as spatial variation of the Bragg

condition, misalignment of the Bragg grating during manufacture, and group-delay ripple across the transverse aperture of the BGFP. An expression for the variation of the effective reflection point can, therefore, be derived as

$$\delta_t = \sqrt{\frac{0.22(d.\delta\nu)^2}{\nu_o^2} - \left[\frac{\lambda^2(1-R)^2}{180R} - \frac{\lambda^2}{D^2}\left\{0.22d^2\theta^2 + \frac{0.08\lambda d}{m}\right\}\right]} \quad (2)$$

where ν_o is the optical frequency, $\delta\nu$ is the required RF resolution, D is the etalon aperture, d is the cavity spacing, R is the nominal reflectivity, λ is the free-space wavelength, and m is the etalon order. It is assumed that each defect contribution has an equal peak excursion across the aperture, as it is unknown what the contributing effect is *a priori*. Thus, a system finesse independent of the BGFP defects would require a peak variation of the reflection point across the aperture of less than 10 nm. This level of fabrication tolerance is difficult to obtain even for a uniformly written interferometric structure.

C. Integrated Optical Lens System

The integrated optical lens system is a means to provide the required phase front to the BGFP in a compact and easily fabricated form. Geometric optics were used in the design of an integrated optical Galilean telescope to expand the beam, and the individual lenses were hybrid diffractive structures designed following [25]. The hybrid structure consists of analog Fresnel regions near the lens center and zone plates where the feature size is less than 2 μm.

III. DESIGN AND FABRICATION

The integrated optical channelizer was fabricated in flame-hydrolysis silica on silicon material. The lenses and waveguides were formed by reactive ion etching to 2 μm and the BGFP was constructed by narrow spatial scanning of a UV beam through a phase mask. The substrate was hypersensitized with 193-nm light to enhance sensitivity and overcome the out diffusion of hydrogen, an approach pioneered in [26]. Post-exposure of the grating was used to align the Fabry–Perot resonance to the peak reflectivity wavelength. The BGFP structure was limited to approximately 10-mm length (including the 1-mm cavity) and a 25-mm aperture to reduce beam walkoff, necessitating a peak reflectivity of approximately 23 dB and an unwanted free spectral range of 150 GHz (40 GHz is preferred, matched to the modulator bandwidth). All other components of the system were standard microwave photonic parts. The waveguide effective index and scalar mode profile were calculated using the eigenvalue solution of Maxwell's equations [27]. An overlap integral method was then used to determine the loss of the lens structures and the focal plane distribution and efficiency were calculated based upon diffraction theory [28]. The BGFP resonance wavelength and bandwidth were calculated based on a numerical implementation of the transfer matrix method (TMM) assuming a single TE polarization and minimal angular dependence [29].
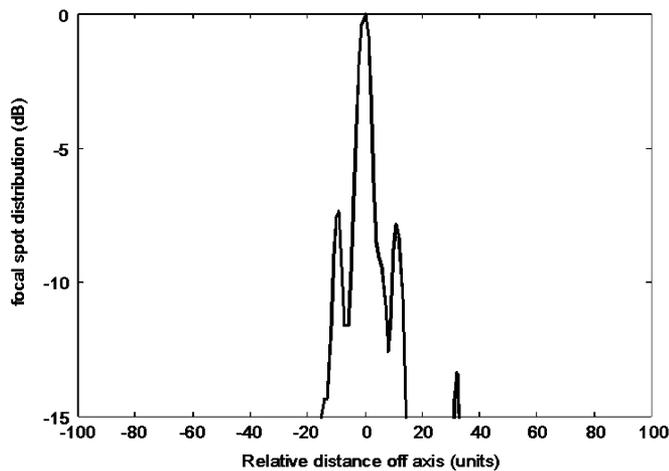
Fig. 3.   IO Lens focal plane distribution.

IV. EXPERIMENTAL RESULTS

A. Integrated Optical Lens System

The focal plane distribution and diffraction efficiency were measured at a wavelength near, but not equal to, the BGFP resonance. The focal point was 103 mm as designed to within experimental error. The sidelobe level and diffraction efficiency were lower than expected values of -8 dB and 58%. The etch depth was measured with a profilometer and the etch depth difference is sufficient to account for the discrepancy between design and fabricated values. The focal plane distribution is shown in Fig. 3. Overall, the lens system is an effective means of providing a compact high-efficiency and wide aperture wavefront to the BGFP.

B. Spectral–Spatial Measurement

Two significant loss mechanisms are apparent in the form of (1): the effect of intracavity loss in the presence of wavelength-dependent reflectivity and the loss associated due to the spreading of the optical power into angular resolution elements. These two effects were found to significantly limit the performance achievable and, thus, a means of calculating the loss contributions from these effects was devised [30]. The spatial distribution of the unmodulated optical signal was measured as a function of laser wavelength. This two-dimensional (2-D) measurement was then reduced to the loss versus wavelength graph shown in Fig. 4 using an approach described in detail in [29].

From the measurements, a single-pass cavity transmission of only $X = 0.9$ is estimated, not excessive, but illustrating the *significant* detrimental effect on the overall loss in excess of 25 dB at the peak wavelength. In addition, the fundamental loss of 15 dB is due to angular power spreading in the Fabry–Perot device. These two loss mechanisms place a limit on the performance that can be achieved with the current design, but provide understanding on how to improve the system frequency resolution.

C. RF Channelizer Demonstration

A channelizer demonstration was nevertheless performed to prove the principle of the integrated optic BGFP as a microwave channelizer. In this measurement, the frequency resolution is
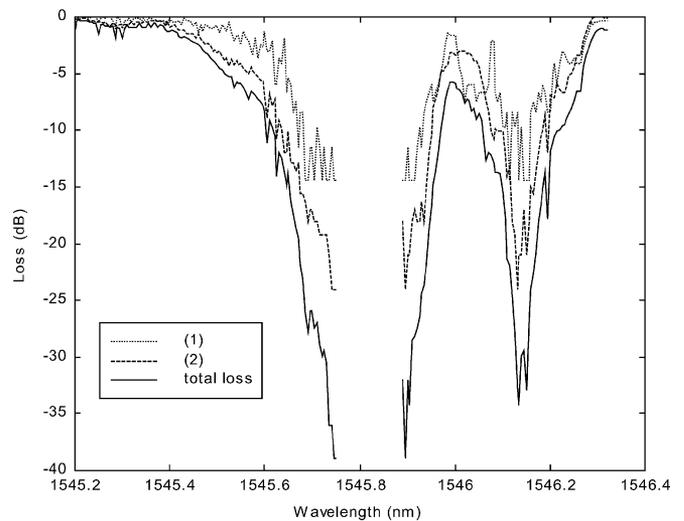

Fig. 4.   BGFP loss via spectral spatial measurement. (1) Loss due to angular power spreading. (2) Loss due to intracavity loss/wavelength dependent reflectivity.
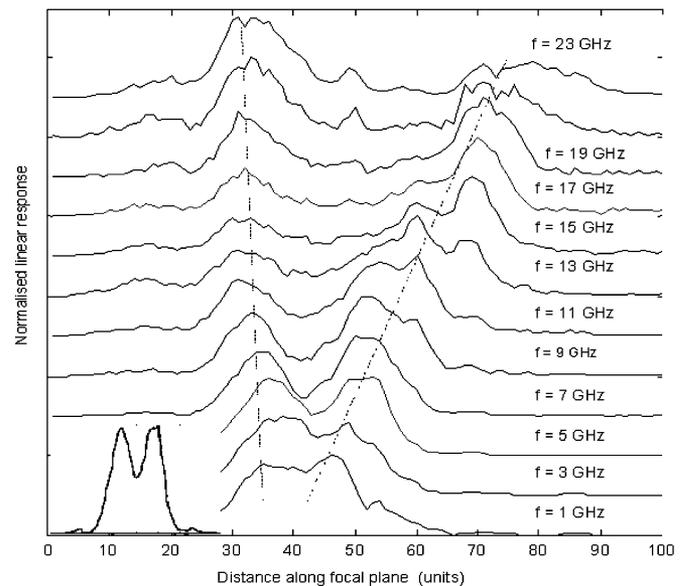

Fig. 5.   Microwave sidebands at focal plane (linear distance units). Inset: sidebands at 5 GHz.

determined by measuring the optically modulated microwave sideband finesse as a function of RF frequency. The modulator was biased at a null to effect double-sideband suppressed carrier (DSB-SC) operation [19], and the laser wavelength was aligned to the point of peak reflectivity. The RF frequency was varied from 1 to 23 GHz so that the sidebands would be spatially demultiplexed across the whole Bragg grating bandwidth. The focal plane intensity distribution was recorded and the results are depicted in Fig. 5. The inset shows the two sideband channels measured at the focal plane for frequency of 5 GHz.

The finesse and loss as a function of RF center frequency are depicted in Fig. 6. The lower sideband has a larger angular dispersion than the upper sideband, which has been noticed in previous experiments [19], and results from the conversion of angular response to the focal plane via the transform lens. The frequency resolution is severely limited by effects described in Sec-
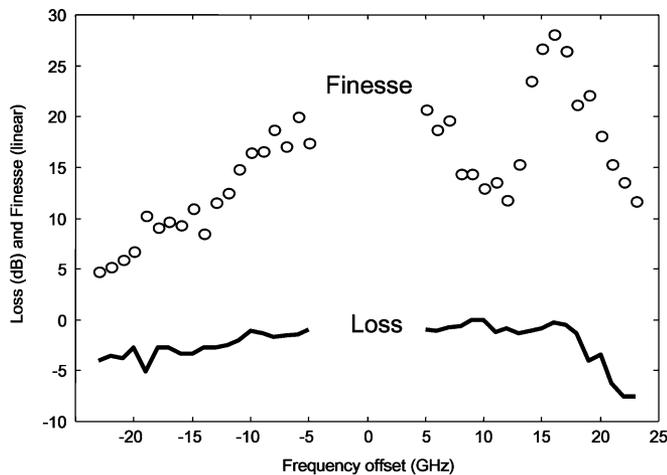
Fig. 6. Finesse and relative loss versus frequency.

tion II-B, but the peak finesse of 27 correlates well between the two measurements. Future designs should take the intracavity loss and wavelength dependent reflectivity into account. Nevertheless, proof-of-principle channelization has been achieved and frequency results are comparable to previous optical channelizer demonstrations in bulk optical form [31].

V. IMPROVEMENTS

The device as demonstrated does not have the resolution expected of a high-performance microwave channelizer. However, the measurements and analysis have provided design insight suitable for such a system. Accurately etching the lens depth or moving to a photosensitive lens [32] will improve the diffraction efficiency and make device fabrication a simple photosensitivity "printing" process. Slight improvements can also be made by tilting the zone plates to maximize efficiency [33]. Extending the phase mask travel to provide a 3.75-mm cavity will reduce the free spectral range to 40 GHz and, thus, increase the frequency resolution by a factor of four. However, the significant loss mechanism was determined to be intracavity loss in the presence of high reflectivity. Increasing the single-pass cavity transmission slightly and matching the required reflectivity will significantly improve performance. Cavity loss can be reduced further with gain in the cavity via erbium-glass materials [34] and, finally, multicavity effects to improve the resolution [35]. The results demonstrated in this study demonstrate the possibility of a channelizer with 40 channels, each with 1-GHz bandwidth covering a 40-GHz range in compact integrated optical form, less than 1500 mm^3 in volume.

VI. CONCLUSION

A means for spatially separating optically modulated RF signals has been described. The method is based on the use of a compact integrated optical BGFP to provide the angular dispersion required for high resolving power of microwave sideband signals. The required input wavefront to the BGFP is provided through the use of a wide aperture hybrid Fresnel lens system integrated onto the substrate. Expressions for the performance limitations of such a device have been derived and a design has been detailed.

The loss mechanisms attributable to the device has been measured and analyzed by a spectral–spatial measurement at the focal plane of the device. Finally, the operation as a channelizer has been demonstrated via a modulated microwave spatial demultiplexing experiment. The etalon finesse varied from 27 to 5 over a 46-GHz spectral range. Suggested limitations and advantages of the approach have been described and the expected performance for a subsequent iteration has been quantified.

REFERENCES

[1] G. W. Anderson, D. C. Webb, A. E. Spezio, and J. N. Lee, "Advanced channelization technology for RF, microwave and millimeterwave applications," *Proc. IEEE*, vol. 79, no. 3, pp. 355–388, Mar. 1991.

[2] C. I. H. Chen, K. George, M. Wang, W. McCormick, and J. B. Y. Tsui, "2.5 GSPS/1 GHz wide band digital receiver," in *Proc. IECON'03*, vol. 2, Nov. 2–6, 2003, pp. 1888–1893.

[3] H. Suzuki, M. Fujiwara, N. Takachio, K. Iwatsuki, T. Kitoh, and T. Shibata, "12.5-GHz spaced 1.28 Tb/s (512-channel × 2.5 Gb/s) super-dense WDM transmission over 320-km SMF using multiwavelength generation technique," *IEEE Photon. Technol. Lett.*, vol. 14, no. 3, pp. 405–408, Mar. 2002.

[4] K. Takada, H. Yamada, and K. Okamoto, "Optical spectrum analyzer using cascaded AWG's with different channel spacings," *IEEE Photon. Technol. Lett.*, vol. 11, no. 7, pp. 863–864, Jul. 1999.

[5] K. Takada, M. Abe, T. Shibata, and K. Okamoto, "1-GHz-spaced 16-channel arrayed-waveguide grating for a wavelength reference standard in DWDM network systems," *J. Lightw. Technol.*, vol. 20, no. 5, pp. 850–853, May 2002.

[6] P. K. Das and C. M. DeCusatis, *Acousto-Optic Signal Processing: Fundamentals and Applications*. Norwood, MA: Artech House, 1991.

[7] T. R. Ranganath, T. R. Joseph, and J. Y. Lee, "The integrated optic spectrum analyzer—A first demonstration," in *Proc. IEEE Int. Electronic Devices Meeting*, Washington, DC, Dec. 1980. Post deadline paper., p. 843.

[8] C. L. Wang and C. S. Tsai, "Integrated magnetooptic Bragg cell modulator in yttrium iron garnet–gadolinium gallium garnet taper waveguide and applications," *J. Lightw. Technol.*, vol. 15, no. 9, pp. 1708–1715, Sep. 1997.

[9] C. Greiner, D. Iazikov, and T. W. Mossberg, "Fourier-transform-limited performance of a lithographically scribed planar holographic Bragg reflector," *IEEE Photon. Technol. Lett.*, vol. 16, no. 3, pp. 840–842, Mar. 2004.

[10] J. Martin, M. Tetu, C. Latrasse, A. Bellemare, and M. Duguay, "Use of a sampled Bragg grating as an in-fiber optical resonator for the realization of a referencing optical frequency scale for WDM communications," in *OFC'97 Tech. Dig.*, 1997, ThJ5, pp. 284–285.

[11] S. Suzuki, M. Yanagisawa, Y. Hibino, and K. Oda, "High-density integrated planar lightwave circuits using SiO2–GeO2 waveguides with a high refractive index difference," *J. Lightw. Technol.*, vol. 12, no. 5, pp. 790–796, May 1994.

[12] D. G. Rabus, M. Hamacher, H. Heidrich, and U. Troppenz, "Box-like filter response of triple ring resonators with integrated SOA sections based on GaInAsP/InP," in *14th InP Rel. Mater. Conf.*, May 12–16, 2002, pp. 479–482.

[13] K. Takada, M. Abe, Y. Hida, T. Shibata, M. Ishii, A. Himeno, and K. Okamoto, "Fabrication of 2 GHz-spaced 16-channel arrayed-waveguide grating demultiplexer for optical frequency monitoring applications," *Electron. Lett.*, vol. 36, no. 19, pp. 1643–1644, Sep. 2000.

[14] H. Yamada *et al.*, "Measurement of phase and amplitude error distributions in arrayed-waveguide grating multi/demultiplexers based on dispersive waveguide," *J. Lightw. Technol.*, vol. 18, no. 9, pp. 1309–1320, Sep. 2000.

[15] W. Wang, R. L. Davis, T. J. Jung, R. Lodenkamper, L. J. Lembo, J. C. Brock, and M. C. Wu, "Characterization of a coherent optical RF channelizer based on a diffraction grating," *IEEE Trans. Microw. Theory Tech.*, vol. 49, no. 10, pp. 1996–2001, Oct. 2001.

[16] S. Xiao *et al.*, "Experimental and theoretical study of hyperfine WDM demultiplexer performance using the virtually imaged phased array (VIPA)," *J. Lightw. Technol.*, vol. 23, no. 3, pp. 1456–1467, Mar. 2005.

[17] S. Janz, A. Balakrishnan, S. Charbonneau, P. Cheben, M. Cloutier, A. Delage, K. Dossou, L. Erickson, M. Gao, P. A. Krug, B. Lamontagne, M. Packirisamy, M. Pearson, and D. X. Xu, "Planar waveguide Echelle gratings in silica-on-silicon," *IEEE Photon. Technol. Lett.*, vol. 16, no. 2, pp. 503–505, Feb. 2004.

[18] J. M. Heaton, C. D. Watson, S. B. Jones, M. M. Bourke, C. M. Boyne, G. W. Smith, and D. R. Wight, "Sixteen-channel (1 to 16 GHz) microwave spectrum analyzer device based on a phased-array of GaAs/Al-GaAs electro-optic waveguide delay lines," in *SPIE Photon. West*, vol. 3278, 1998, pp. 30–32.

[19] E. Hecht, *Optics*. Reading, MA: Addison-Wesley, 1987.

[20] E. M. Alexander and R. W. Gammon, "The Fabry–Perot etalon as an RF frequency channelizer," *Proc. SPIE–Int. Soc. Opt. Eng.*, vol. 464, pp. 45–52, 1984.

[21] W. Dawber and K. Webster, "Electro-optical microwave signal processor for high frequency wide-band frequency channelization," *Proc. SPIE–Int. Soc. Opt. Eng.*, vol. 3388, pp. 77–88, 1998.

[22] K. Noguchi, O. Mitomi, and H. Miyazawa, "Millimeter-wave $Ti:LiNbO_3$ optical modulators," *J. Lightw. Technol.*, vol. 16, no. 4, pp. 615–619, Apr. 1998.

[23] G. Hernandez, *Fabry–Perot Interferometers*. Cambridge, U.K.: Cambridge Univ. Press, 1986.

[24] A. Yariv, *Optical Waves in Crystals*. New York: Wiley, 1984.

[25] T. Suhara and H. Nishihara, "Integrated optics components and devices using periodic structures," *IEEE J. Quantum Electron.*, vol. QE-22, no. 6, pp. 337–359, Jun. 1986.

[26] M. Aslund, J. Canning, and G. Yoffe, "Locking in photosensitivity within optical fiber and planar waveguides by ultraviolet pre-exposure," *Opt. Lett.*, vol. 24, no. 25, pp. 1826–1828, Dec. 1999.

[27] C. M. Kim and R. V. Ramaswamy, "Modeling of graded index channel waveguides using nonuniform finite difference method," *J. Lightw. Technol.*, vol. 7, no. 10, pp. 1581–1589, Mar. 1989.

[28] T. Q. Vu, C. S. Tsai, and Y. C. Kao, "Integration of a curved hybrid waveguide lens and photodetector array in a GaAs waveguide," *Appl. Opt.*, vol. 31, no. 25, pp. 5246–5254, Sep. 1992.

[29] M. Yamada and K. Sakuda, "Analysis of almost periodic distributed feedback slab waveguides via a fundamental matrix approach," *Appl. Opt.*, vol. 26, no. 16, pp. 3474–3478, 1987.

[30] S. T. Winnall, "Microwave photonic receivers for electronic warfare applications," Ph.D. dissertation, Roy. Melbourne Inst. Technol., Melbourne, Australia, 2001.

[31] E. M. Alexander, "Optical techniques for wide bandwidth spectrum analysis," *Proc. SPIE–Int. Soc. Opt. Eng.*, vol. 789, pp. 169–175, 1987.

[32] J. Albert, J. Huttunen, and J. Saarinen, "Planar Fresnel lens photoimprinted in a germanium-doped silica optical waveguide," *Opt. Lett.*, vol. 20, no. 10, pp. 1136–1138, 1995.

[33] Z. Q. Lin, S. T. Zhou, W. S. C. Chang, S. Forouhar, and J. M. Delavaux, "A generalized two-dimensional coupled-mode analysis of curved and chirped periodic structures in open dielectric waveguides," *IEEE Trans. Microw. Theory Tech.*, vol. MTT-29, no. 9, pp. 881–891, Sep. 1981.

[34] S. Guldberg-Kjaer, J. Hubner, M. Kristensen, C. Laurent-Lund, M. Rysholt-Poulsen, and M. W. Sckerl, "Planar waveguide laser in Er/Al-doped germanosilicate," *Electron. Lett.*, vol. 35, no. 4, pp. 302–303, Feb. 1999.

[35] H. van de Stadt and J. M. Miller, "Multimirror Fabry–Perot interferometers," *J. Opt. Soc. Amer. A, Opt. Image Sci.*, vol. 2, no. 8, pp. 1363–1370, Aug. 1985.

A. C. Lindsay (M'90), photograph and biography not available at time of publication.

Michael W. Austin (M'83) received the B.Eng. degree in communication engineering and M.Eng. degree from the Royal Melbourne Institute of Technology (RMIT), Melbourne, Victoria, Australia, in 1977 and 1980 respectively, and the Ph.D. degree in electronic engineering from the University of London, London, U.K., in 1982. His Ph.D. dissertation concerned the fabrication of curved optical waveguides in GaAs/GaAlAs.

From 1979 to 1982, he was a Research Fellow with British Telecom Research Laboratories, Ipswich, U.K., where he was involved in the field of integrated optics in III–V semiconductor materials. Since 1982, he has been a member of the academic staff with the Department of Communication and Electronic Engineering (now the School of Electrical and Computer Engineering), RMIT University. Since 1994, he has been the Director of the Microelectronics and Materials Technology Centre (MMTC), RMIT. He is also the Program Manager for the Photonic Information Processing Research Program with the Australian Photonics Cooperative Research Centre. His research interests include the theoretical and experimental study of planar optical waveguide devices, particularly the fabrication of wide-band optical intensity modulators in lithium niobate.

Prof. Austin is a Fellow of the Institution of Engineers, Australia.

John Canning (M'98) is currently the Group Leader in gratings, photonic crystal fiber, sensors and lasers with the Optical Fiber Technology Centre (OFTC), University of Sydney, Eveleigh, N.S.W., Australia. He founded the photonic crystal fiber fabrication work at the OFTC and is inventor of the Fresnel fiber. He has been involved with planar and fiber technologies, particularly gratings, both passive and active, as well as other devices including photonic crystal fiber lasers and microfluidic electronics. He was involved with the establishment of a number of spinoff companies using these technologies, the most recent being Centaurus Technologies Pty Ltd. He has authored or coauthored over 250 journal and conference publications. He holds over 25 patents in relevant areas covering largely silica and polymer material platforms.

Steve T. Winnall (M'94) received the B.Eng. degree in electrical and electronic engineering from the University of Adelaide, Adelaide, Australia, in 1994, and the Ph.D. degree (in the area of microwave photonic receivers for electronic warfare applications) from the Royal Melbourne Institute of Technology (RMIT), Melbourne, Victoria, Australia, in 2002.

From 1994 to 2001, he was with the Defence Science and Technology Organization, Department of Defence, where he was involved in the area of advanced microwave and photonic devices and systems. From 2001 to 2004, he was with Redfern Broad-Band Networks Inc., where he designed and manufactured their state-of-the art optical networking equipment. He is currently the Electrical Team Leader with Cochlear Ltd., Land Cover, N.S.W., Australia. His research interests include RF and microwave electronics and signal processing.

Arnan Mitchell (S'97–M'00) was born in Dublin, Ireland, on February 20, 1973. He received the B.Tech. degree (with honors) in opto-electronics from Macquarie University, Sydney, Australia, in 1993, and the Ph.D. degree from the Royal Melbourne Institute of Technology (RMIT), Melbourne, Victoria, Australia. He was an Australian Photonics CRC Research Fellow with RMIT, where he investigated broad-band and specialized integrated optical modulators and RF photonic components for communications and signal-processing applications. He is currently a Senior Lecturer with the School of Electrical and Computer Engineering, RMIT. He maintains an active interest in the research of numerical methods required for the design of RF photonic integrated devices.